Origin of the p-Type Character of $AuCl_3$ Functionalized Carbon Nanotubes

Altynbek Murat,[†] Ivan Rungger,[‡] Chengjun Jin,[†] Stefano Sanvito,[‡] and Udo Schwingenschlögl[*,†]

PSE Division, KAUST, Thuwal 23955-6900, Kingdom of Saudi Arabia, and School of Physics and CRANN, Trinity College, Dublin 2, Ireland

E-mail: udo.schwingenschlogl@kaust.edu.sa,+966(0)544700080

Abstract

The microscopic origin of the p-type character of $AuCl_3$ functionalized carbon nanotubes (CNTs) is investigated using first-principles self-interaction corrected density functional theory (DFT). Recent DFT calculations suggest that the p-type character of $AuCl_3$ functionalized CNTs is due to the Cl atoms adsorbed on the CNTs. We test this hypothesis and show that adsorbed Cl atoms only lead to a p-type character for very specific concentrations and arrangements of the Cl atoms, which furthermore are not the lowest energy configurations. We therefore investigate alternative mechanisms and conclude that the p-type character is due to the adsorption of $AuCl_4$ molecules. The unraveling of the exact nature of the p-doping adsorbates is a key step for further development of $AuCl_3$ functionalized CNTs in water sensor applications.

Keywords: p-type doping, CNT, sensor, chemical functionalization

[†]PSE Division, KAUST, Thuwal 23955-6900, Kingdom of Saudi Arabia
[‡]School of Physics and CRANN, Trinity College, Dublin 2, Ireland

Introduction

Carbon nanotubes (CNTs) have a wide range of applications in transistors, spintronics, sensors, and solar cells.[1–7] Due to their "quantum nature" and high surface-to-volume ratio, they are considered as promising candidates for extremely sensitive gas sensors.[3,8–10] However, the gas sensing response of pristine CNTs is weak due to the strong sp^2 bonds of the carbon network, characterized by a low chemical reactivity. Thus, functionalization of the CNT surface is necessary to obtain a gas sensor with high sensitivity and selectivity.

Recently, $AuCl_3$ functionalized semiconducting CNTs have been experimentally investigated.[11,12] It has been found that the system exhibits a selective H_2O adsorption and is insensitive to O_2 and N_2 gases. This is advantageous for designing selective water sensors. Moreover, a p-type character of the semi-conducting CNTs is observed when functionalized with $AuCl_3$,[11,13] where the Fermi energy is found to lie just below the top of the valence band maximum and no defect states appear inside the CNT band gap,[13] which is of general importance for fabricating nanoscale devices.

The crystal structure of $AuCl_3$ consists of stacked planar Au_2Cl_6 molecules.[14] Au_2Cl_6 exists as a chloride-bridged Au dimer at low temperatures where each Au center is surrounded by four Cl atoms in a square planar configuration. When dissolved, $AuCl_3$ can have different ionic conformations depending on the coordinating agent. In the experiments in Refs. 11 and 12 nitromethane is used as solvent, in which $AuCl_3$ can be dissolved into single atoms, Au^{3+} and Cl^-, and at the same time $AuCl_4^-$ molecular ions can be formed.[15,16] It has been suggested, both experimentally[11,12] and theoretically[17] that the Cl anions are the origin of the observed p-type behavior of $AuCl_3$ doped CNTs and that the Au cations and $AuCl_4$ molecules do not play a significant role. This scenario has been examined by density functional theory (DFT) calculations[17] and it was found that the CNT-Cl system shows p-type behavior due to a shift of the Fermi level towards the valence band.

In this work we perform DFT calculations with the aim to compare possible reasons for the p-type character observed in $AuCl_3$ functionalized CNTs. We study the formation and adsorption of the different conformations of $AuCl_3$ in nitromethane. In addition to doping with isolated atoms, we also study Au-Cl molecules attached to the CNT, in particular $AuCl_4$ and Au_2Cl_6. The elec-

tronic band structures and densities of states obtained for the different configurations are compared to available experimental data, which points to an alternative explanation of the experimentally achieved p-type doping not based on individual Cl atom adsorption.

Methods

In our calculations we use a (10,0) semiconducting CNT corresponding to that of Ref. 17. One primitive unit cell contains 40 atoms. We use a supercell containing 80 carbon atoms with a cell size of $30\times30\times17$ Å^3. Electronic structure calculations are performed using the SIESTA implementation of the first-principles DFT formalism.[20] A double-ζ polarized atomic orbital basis set for C, Au, and Cl is used together with the Troullier-Martins scheme for constructing norm-conserving pseudopotentials.[21] A plane wave cutoff of 250 Ry is chosen for the real space grid and the Brillouin zone is sampled with a $1\times1\times4$ Monkhorst-Pack k-point grid. Periodic boundary conditions are applied and sufficient vacuum is used in all calculations to avoid interaction between periodic images. In the structural relaxations all atoms in the unit cell are allowed to move until the atomic forces are less than 0.03 eV/Å. Both the generalized gradient approximation (GGA)[22] and local-density approximation (LDA) are used to optimize the above structures and to obtain the electronic structures. We find that the GGA and LDA essentially give the same results. However, it is known that the LDA overestimates the electron delocalization, especially for dilute doping.[24] Therefore, the LDA alone can be misleading for describing the localized defect band in the doped system. Different advanced techniques can be used to improve the description of electron-electron interactions. Here we use the atomic self-interaction correction (ASIC),[25] which also corrects for the overestimated delocalization of the LDA and generally improves the band alignment in defective systems.[26,27] To investigate the effect of the ASIC, we use different values for the scaling parameter α, which controls the amount of ASIC added and can go from 0.0 (pure LDA) to 1.0 (full ASIC). The general trend is that with increasing α the occupied defect states move down in energy with respect to the CNT states. The discussion of our results is based on ASIC calculations

with α=0.5, which is typically appropriate for defects in extended semiconducting systems, but it is mentioned whenever LDA and full ASIC differ significantly.

Results and Discussion

Role and formation of single Cl atoms

First, we investigate the electronic structure of Cl doped CNTs. In particular, we study the effect of different concentrations of Cl atoms attached on top of the C atoms as well as the dependence of the results on the relative positions of the Cl atoms. Figure Figure 1 presents the electronic band structures of pristine and Cl doped CNTs for different concentrations and configurations (ASIC, $\alpha = 0.5$). Figure Figure 1a shows for the pristine CNT a band gap of 0.8 eV with the Fermi energy in the middle of the band gap, in good agreement with previous DFT calculations.[18,19]

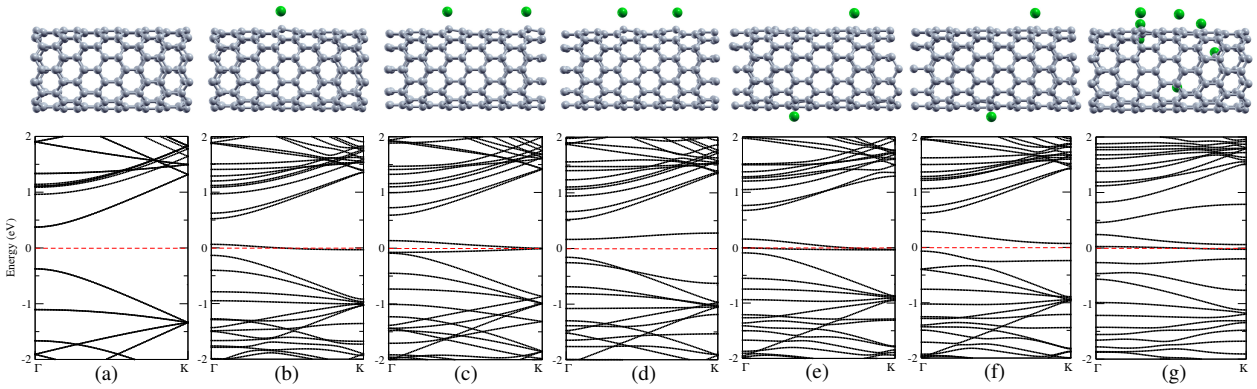

Figure 1: (Color online) Electronic band structure of CNTs: (a) pristine, (b) one Cl doped, (c) two equidistant Cl doped, (d) two non-equidistant Cl doped, (e, f) two Cl doped on different sides with different distances, and (g) seven Cl doped.

When the CNT is doped with a low concentration of one Cl atom per cell the band structure shows a distinct band around the Fermi energy, see Figure Figure 1b. This can be interpreted as a p-type system. Figure Figure 1c shows the band structure for two Cl atoms with a specific arrangement, where a cell of half the size with one Cl atom is doubled along the CNT axis. The smaller cell corresponds to that in Figure 1 in Ref. 17. The band structure in Figure Figure 1c is in agree-

ment with the results in Ref. 17 and does indicate a p-type character for this Cl concentration. Note that the calculations addressed in Figure Figure 1 are performed without spin-polarization. Due to the high DOS at the Fermi energy, spin-polarized calculations results in a small spin-splitting, where an increasing α leads to an increasing spin-polarization due to the enhanced localization of the states. However, another and more effective way for the system to reduce the DOS at the Fermi energy, and thereby the total energy, is a Peierls-type distortion, where the two neighboring Cl atoms undergo small shifts so that the periodicity is broken. Peierls-type distortions in semiconducting and metallic CNTs have been extensively studied,[28–31] while we only consider Peierls-type distortions of the Cl adatoms. This situation is realized in Figure Figure 1d. It can be seen that due to the broken periodicity a gap opens at the Fermi energy and we obtain occupied bonding states and empty antibonding states. Therefore, no p-type behavior is encountered for the same Cl concentration as in Figure Figure 1c. Importantly, the total energy of this second system is by about 0.6 eV lower than for the perfectly periodic system, reflecting the Peierls-type instability. As a further example of an equidistant arrangement, in Figure Figure 1e the two Cl atoms are placed on opposite sides of the CNT (but still equidistant along the CNT axis). Therefore the interaction between them is minimized. The resulting band structure is similar to Figure Figure 1c. When we again slightly shift one of the Cl atoms along the CNT axis a band gap opens at the Fermi energy, see Figure Figure 1f, accompanied by a reduction of the total energy by 1.7 eV. Overall, the system in Figure Figure 1d has the lowest energy of the considered two-Cl configurations, with the energy of the system in Figure Figure 1f being only marginally higher by 0.2 eV. Note that in all the cases there is only a minimal charge transfer between Cl and the CNT, with the Cl atoms remaining essentially charge neutral. Our results show that the recent conclusion that Cl atoms are the origin of the p-type doping[11,12,17] is only valid for very specific high-energy configurations and concentrations. For random or generally low-energy Cl configurations we obtain filled and empty defect states rather than a shift of the Fermi energy below the CNT valence band maximum, which contradicts experimental evidence.[13,17]

Finally, in Figure Figure 1g we show the band structure for a very high local Cl concentration,

where seven Cl atoms have been adsorbed on the upper side of the CNT. At this concentration and for this specific configuration the number of defect bands is so large that they essentially close the CNT band gap and make the system metallic. A substantial reduction of the gap is already observed for the cells with two Cl atoms, especially for the low energy asymmetric arrangements, see Figure Figure 1d and Figure Figure 1f. Such a gap closure contradicts the experimental preservation of the band gap for $AuCl_3$ functionalized CNTs and further corroborates our conclusion that individual Cl atoms are not responsible for the observed p-type character.

Electronic properties for Au_2Cl_6 and $AuCl_4$ adsorption

Having established that individual Cl atoms cannot explain the p-type character, we investigate other possible sources. Using x-ray photoelectron spectroscopy, the different species attached to the CNT after immersion in $AuCl_3$ solution and subsequent drying have been determined in Ref. 12. It has been found that at room temperature there are both neutral Au atoms on the CNT as well as Au^{3+} ions, in approximately the same amount. Visual characterization proves the presence of Au clusters, which allows us to conclude that the neutral Au atoms are mostly combined to larger clusters. To be in a 3+ state the Au atoms need to be coordinated by negatively charged Cl ions, which indicates that charged Au is most likely found in the presence of Au_2Cl_6 and/or $AuCl_4$ molecules, since $AuCl_3$ is much less stable.[14,15] With increasing temperature the amount of Au^{3+} is found to decrease, whereas the amount of neutral Au increases. At the same time, the size and number of Au clusters is found to increase with temperature, whereas the Cl signal decreases with temperature.[12] These results indicate that the energy added to the system by the temperature leads to a breaking of the molecules into their constituents. The individual Au atoms do not desorb from the CNT but move along it until they merge with an Au cluster, which increases the cluster size. The Cl atoms on the other hand can form Cl_2 molecules and desorb.

To confirm this picture, we calculate the formation energies for individual Cl and Au atoms on

the CNT. The formation energy is defined as

$$E_{\text{form,Cl}} = E_{\text{CNT+Cl}} - E_{\text{CNT}} - 1/2E_{\text{Cl}_2}, \quad (1)$$

$$E_{\text{form,Au}} = E_{\text{CNT+Au}} - E_{\text{CNT}} - E_{\text{Au,bulk}}. \quad (2)$$

Here, E_{CNT} is the energy of the isolated CNT, $E_{\text{CNT+Cl}}$ ($E_{\text{CNT+Au}}$) is the energy of the CNT with the adsorbed Cl (Au) atom, E_{Cl_2} is the total energy of a Cl_2 molecule, and $E_{\text{Au,bulk}}$ is the energy of bulk Au per atom. We obtain $E_{\text{form,Cl}} = 0.4$ eV and $E_{\text{form,Au}} = 3.3$ eV. These positive values indicate that for Cl it is more favorable to form Cl_2 molecules rather than being attached as individual atoms to the CNT and that for Au it is favorable to form clusters. We also evaluate the energy for Au atoms to migrate along the CNT using the nudged elastic band method and find an energy barrier of 75 meV, which is easily activated by thermal energy at the experimental conditions. The migration path is along the zigzag direction of the C bond and the adsorption position is on top of a C atom, with a bond length of 2.2 Å. These results are consistent with the experimental observation of Au cluster formation and Cl_2 desorption with increasing temperature.[12]

Interestingly, experimentally also the conductance is found to decrease with increasing temperature,[12] implying that the conductance of the $AuCl_3$–doped CNT is proportional to the Au^{3+} and Cl concentrations. It also excludes Au clusters playing a significant role, since those are found also at high temperature. Combined with the results from the previous section, namely that also individual Cl atoms cannot be responsible for the observed p-type character and preserved band gap, the most likely candidates are Au_2Cl_6 and $AuCl_4$ molecules adsorbed on the CNT.

Before analyzing their electronic structure, we first estimate the binding energies of the molecules to the CNT. The binding energy is defined as

$$E_{\text{b}} = E_{\text{CNT+mol}} - E_{\text{CNT}} - E_{\text{mol}}, \quad (3)$$

where E_{CNT} and E_{mol} are the energies of the isolated CNT and molecules, respectively, and $E_{\text{CNT+mol}}$ is the total energy of the combined system. We obtain for $AuCl_4$ and Au_2Cl_6 bind-

ing energies of -1.6 eV and -0.6 eV, respectively. These rather large negative values show that the molecules bind strongly to the CNT, especially $AuCl_4$. We find that both Au_2Cl_6 and $AuCl_4$ physically adsorb on the CNT without any significant structural distortion, at a binding distance of 3 Å. Our calculated band structure of a single Au_2Cl_6 molecule attached to the CNT is shown in Figure Figure 2a. The CNT bands are essentially unperturbed by the molecule, compare Figure Figure 1a, and the Au_2Cl_6 bands show almost no dispersion, indicating that they are localized on the molecule and do not hybridize with the C states. No p-type behavior is found but rather localized gap states at different energies, which depend on the Au_2Cl_6 concentration.

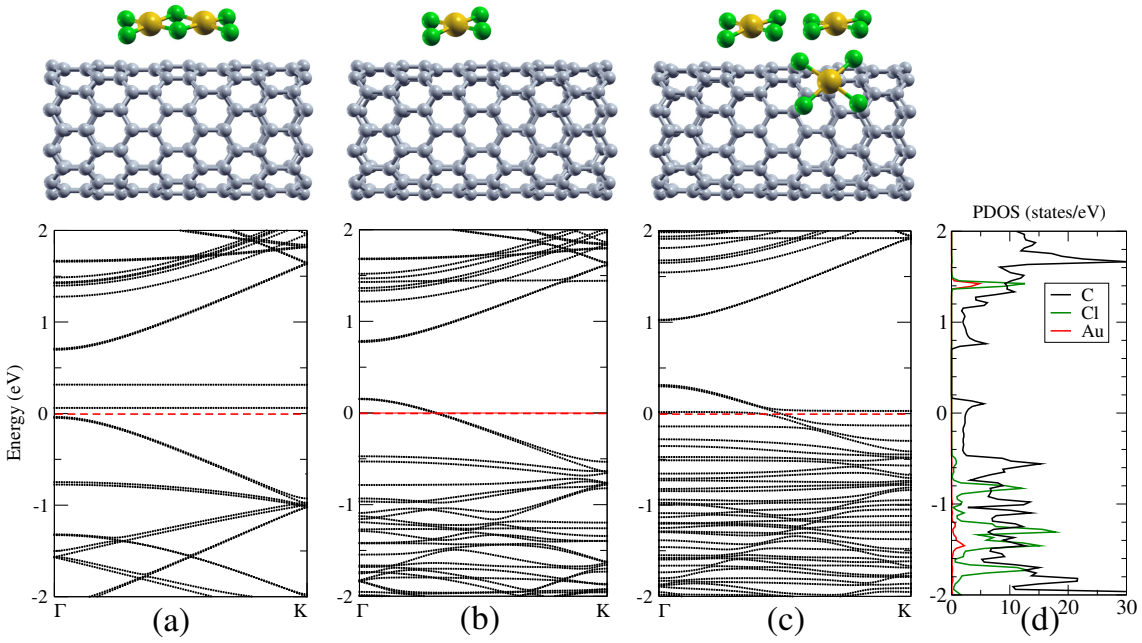

Figure 2: (Color online) Electronic band structure of CNTs doped with different molecules as calculated with ASIC $\alpha = 0.5$: (a) Au_2Cl_6, (b) one $AuCl_4$, (c) three $AuCl_4$, and (d) density of states for case (b).

The band structure of a single $AuCl_4$ molecule attached to the CNT is shown in Figure Figure 2b. It indicates a p-type behavior, where the Fermi energy is shifted below the valence band maximum of the CNT due to charge transfer of a full electron to the $AuCl_4$. To compare the effect of ASIC, Figure Figure 3 presents the electronic band structure of the CNTs doped with one $AuCl_4$ molecule, calculated with $\alpha = 0$ (pure LDA), $\alpha = 0.5$, and $\alpha = 1$ (full ASIC). Indeed, as expected, the general trend is that with increasing α the occupied defect states move down in energy with

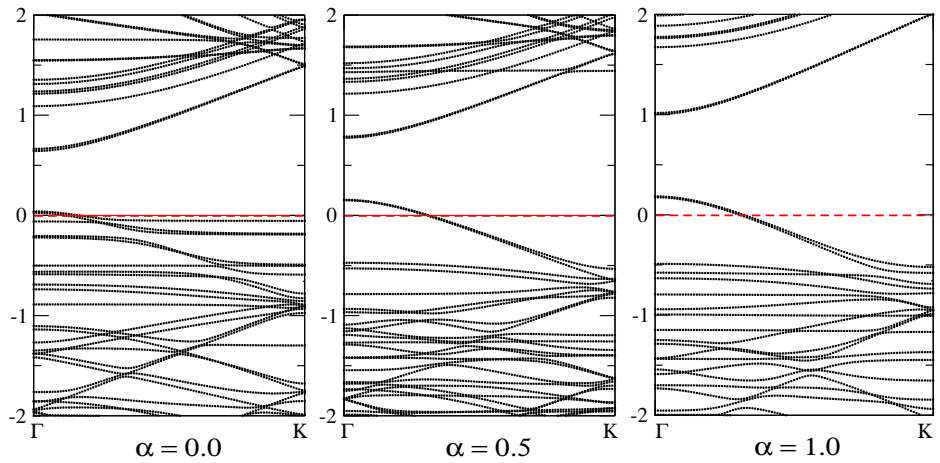

Figure 3: (Color online) Electronic band structures of CNTs doped with one $AuCl_4$ molecule, calculated with $\alpha = 0$ (pure LDA), $\alpha = 0.5$, and $\alpha = 1$ (full ASIC).

respect to the CNT states. ASIC with $\alpha = 0.5$ increases the band gap of the pure LDA by 0.1 eV and $\alpha = 1$ increases it by further 0.3 eV. Long-range corrected functionals as investigated in Ref. 23 are expected not to modify our conclusions, because already the ASIC does not result in qualitative changes as compared to the LDA. The occupied molecular states are resonant with the valence band of the pristine CNT and show little dispersion, indicating rather localized states. This is further confirmed by the projected density of states, see Figure Figure 2d, where it is seen that the Cl states are all occupied, whereas the C states are partly empty at the valence band maximum. These findings are in good agreement with experiment. We thus conclude that the $AuCl_4$ molecules are responsible for the observed p-type character and associated conductance properties.[11,12] We plot the HOMO and LUMO wave functions for the CNT doped with one $AuCl_4$ molecule as calculated with $\alpha = 0.5$ at the Γ point in Figure Figure 4. The LUMO+1, LUMO, HOMO, and HOMO-1 are localized on the CNT whereas, the HOMO-2 is localized on the molecule. Only the HOMO shows slight hybridization with the molecule. The LDA HOMO is the ASIC $\alpha = 0.5$ HOMO-2 which is consistent with the increased localization due to the self-interaction reduction. As expected the states associated with p-type doping in Figure Figure 1 are mostly localized on the CNTs. Moreover, a Mulliken population analysis shows that the net charge transfer between the CNT and the single $AuCl_4$ is 0.44 e^- which is higher than the highest net charge transfer of 0.17 e^- among the

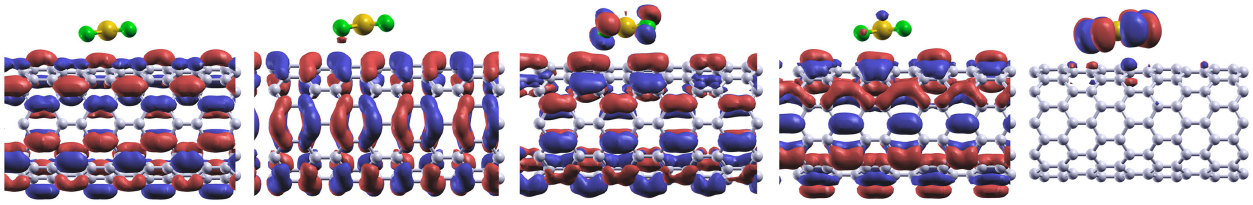

Figure 4: (Color online) HOMO and LUMO wave function isosurfaces of the CNT doped with one $AuCl_4$ molecule, calculated with $\alpha = 0.5$.

cases with two doped Cl atoms, Figure Figure 1c. We further investigate the effect of increasing the $AuCl_4$ concentration on the band structure. As presented in Figure Figure 2c, we find that when more $AuCl_4$ molecules are attached to the CNT in close proximity, specifically three closely spaced molecules, the p-type behavior is preserved. The band gap is also preserved, in contrast to what happens for higher concentrations of isolated Cl atoms, see Figure Figure 1g. For high concentrations the CNT, however, cannot provide one full electron for each molecule, so that the highest molecular states are now located around the Fermi energy, but well below the CNT valence band maximum.

Conclusions

In conclusion, we have investigated the origin of the experimentally observed p-type character of $AuCl_3$ functionalized CNTs. We have shown that individual Cl atoms cannot account for the p-type doping, contrary to previous claims in the literature, and therefore propose an alternative explanation. In particular, we have studied the possible formation of different conformations of $AuCl_3$ as well as the effect of different adsorbate concentrations. We find that especially $AuCl_4$ molecules bind strongly to the CNT and that they lead to an electron transfer from the CNT to the molecules and thus a shift of the Fermi energy below the valence band maximum. We conclude that the origin of the p-type doping in $AuCl_3$ functionalized CNT is $AuCl_4$ adsorption, which is key in understanding the mechanisms behind the resistivity changes in water vapor sensors based on $AuCl_3$ functionalized CNTs.

Acknowledgement

Financial support and computational resources have been provided by King Abdullah University of Science and Technology (ACRAB project). Calculations have been performed on the Shaheen supercomputer and Noor Linux cluster.

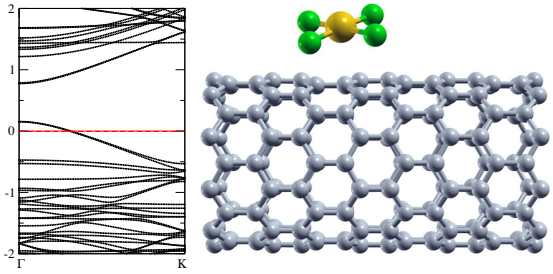

References

(1) Tans, S. J.; Verschueren, A. R. M.; Dekker, C. Room-Temperature Transistor Based on a Single Carbon Nanotube. *Nature* **1998**, *393*, 49–52.

(2) Zhou, C.; Kong, J.; Yenilmez, E.; Dai, H. Modulated Chemical Doping of Individual Carbon Nanotubes. *Science* **2000**, *290*, 1552–1555.

(3) Goldoni, A.; Petaccia, L.; Lizzit, S.; Larciprete, R. Sensing Gases with Carbon Nanotubes: a Review of the Actual Situation. *J. Phys.: Condens. Matter* **2010**, *22*, 013001.

(4) Kuemmeth, F.; Churchill, H.; Herring, P.; Marcus, C. Carbon Nanotubes for Coherent Spintronics. *Materials Today* **2010**, *13*, 18–26.

(5) Lee, J. M.; Kwon, B. H.; Park, H.; Kim, H.; Kim, M. G.; Park, J. S.; Kim, E. S.; Yoo, S.; Jean, D. Y.; Kim, S. O. Exciton Dissociation and Charge-Transport Enhancement in Organic Solar Cells with Quantum-Dot/N-Doped CNT Hybrid Nanomaterials. *Advanced Materials* **2013**, *25*, 2011–2017.

(6) Lu, L.; Xu, T.; Chen, W.; Lee, J. M.; Luo, Z.; Jung, I. H.; Park, H.; Kim, S. O.; Yu, L. The

Role of N-Doped Multiwall Carbon Nanotubes in Achieving Highly Efficient Polymer Bulk Heterojunction Solar Cells. *Nano Letters* **2013**, *13*, 2365–2369.

(7) Lee, J. M.; Park, J. S.; Lee, S. H.; Kim, H.; Yoo, S.; Kim, S. O. Selective Electron- or Hole-Transport Enhancement in Bulk-Heterojunction Organic Solar Cells with N- or B-Doped Carbon Nanotubes. *Advanced Materials* **2011**, *23*, 629–633.

(8) Zhang, T.; Mubeen, S.; Myung, N. V.; Deshusses, M. A. Recent Progress in Carbon Nanotube-Based Gas Sensors. *Nanotechnology* **2008**, *19*, 332001.

(9) Peng, S.; Cho, K. Ab Initio Study of Doped Carbon Nanotube Sensors. *Nano Lett.* **2003**, *3*, 513–517.

(10) Zanolli, Z.; Leghrib, R.; Felten, A.; Pireaux, J.-J.; Llobet, E.; Charlier, J.-C. Gas Sensing with Au-Decorated Carbon Nanotubes. *ACS Nano* **2011**, *5*, 4592–4599.

(11) Lee, I. H.; Kim, U. J.; Son, H. B.; Yoon, S. M.; Yao, F.; Yu, W. J.; Duong, D. L.; Choi, J. Y.; Kim, J. M.; Lee, E. H. et al. Hygroscopic Effects on $AuCl_3$-Doped Carbon Nanotubes. *J. Phys. Chem. C* **2010**, *114*, 11618–11622.

(12) Kim, S. M.; Kim, K. K.; Jo, Y. W.; Park, M. H.; Chae, S. J.; Duong, D. L.; Yang, C. W.; Kong, J.; Lee, Y. H. Role of Anions in the $AuCl_3$-Doping of Carbon Nanotubes. *ACS Nano* **2011**, *5*, 1236–1242.

(13) Kim, K. K.; Bae, J. J.; Park, H. K.; Kim, S. M.; Geng, H. Z.; Park, K. A.; Shin, H. J.; Yoon, S. M.; Benayad, A.; Choi, J. Y. et al. Fermi Level Engineering of Single-Walled Carbon Nanotubes by $AuCl_3$ Doping. *JACS* **2008**, *130*, 12757–12761.

(14) Clark, E. S.; Templeton, D. H.; MacGillavry, C. H. The Crystal Structure of Gold(III) Chloride. *Acta Crystallographica* **1958**, *11*, 284–288.

(15) Abdou, M. S.; Holdcroft, S. Oxidation of π-Conjugated Polymers with Gold Trichloride:

Enhanced Stability of the Electronically Conducting State and Electroless Deposition of Au^0. *Synth. Met.* **1993**, *60*, 93–96.

(16) Kim, K. K.; Yoon, S. M.; Park, H. K.; Shin, H. J.; Kim, S. M.; Bae, J. J.; Cui, Y.; Kim, J. M.; Choi, J. Y.; Lee, Y. H. Doping Strategy of Carbon Nanotubes with Redox Chemistry. *New J. Chem.* **2010**, *34*, 2183–2188.

(17) Duong, D. L.; Lee, I. H.; Kim, K. K.; Kong, J.; Lee, S. M.; Lee, Y. H. Carbon Nanotube Doping Mechanism in a Salt Solution and Hygroscopic Effect: Density Functional Theory. *ACS Nano* **2010**, *4*, 5430–5436.

(18) Reich, S.; Thomsen, C.; Ordejón, P. Electronic Band Structure of Isolated and Bundled Carbon Nanotubes. *Phys. Rev. B* **2002**, *65*, 155411.

(19) Chen, C. W.; Lee, M. H.; Clark, S. J. Band Gap Modification of Single-Walled Carbon Nanotube and Boron Nitride Nanotube Under a Transverse Electric Field. *Nanotechnology* **2004**, *15*, 1837–1843.

(20) Soler, J.; Artacho, E.; Gale, J.; García, A.; Junquera, J.; Ordejón, P.; Sánchez-Portal, D. The SIESTA Method for Ab Initio Order-N Materials Simulation. *J. Phys.: Condens. Matter* **2002**, *14*, 2745–2779.

(21) Delley, B. An All-Electron Numerical Method for Solving the Local Density Functional for Polyatomic Molecules. *J. Chem. Phys.* **1990**, *92*, 508.

(22) Perdew, J.; Burke, K.; Ernzerhof, M. Generalized Gradient Approximation Made Simple. *Phys. Rev. Lett.* **1996**, *77*, 3865.

(23) Ramirez, J.; Mayo, M. L.; Kilina, S.; Tretiak, S. Electronic Structure and Optical Spectra of Semiconducting Carbon Nanotubes Functionalized by Diazonium Salts . *Chem. Phys.* **2013**, *413*, 89–101.

(24) Kohanoff, J. in *Electronic Structure Calculations for Solids and Molecules: Theory and Computational Methods*; Cambridge University Press, 2006; pp 75–120.

(25) Pemmaraju, C.; Archer, T.; Sanchez-Portal, D.; Sanvito, S. Atomic-Orbital-Based Approximate Self-Interaction Correction Scheme for Molecules and Solids. *Phys. Rev. B* **2007**, *75*, 045101.

(26) Droghetti, A.; Pemmaraju, C. D.; Sanvito, S. Predicting d^0 Magnetism: Self-Interaction Correction Scheme. *Phys. Rev. B* **2008**, *78*, 140404(R).

(27) Pemmaraju, C. D.; Hanafin, R.; Archer, T.; Braun, H. B.; Sanvito, S. Impurity-Ion Pair Induced High-Temperature Ferromagnetism in Co-Doped ZnO. *Phys. Rev. B* **2008**, *78*, 054428.

(28) Torres, L. E. F. F.; Roche, S. Inelastic Quantum Transport and Peierls-Like Mechanism in Carbon Nanotubes. *Phys. Rev. Lett.* **2006**, *97*, 076804.

(29) Rafailov, P. M.; Janina, M.; Christian, T.; Hiromichi, K. Electrochemical Switching of the Peierls-Like Transition in Metallic Single-Walled Carbon Nanotubes. *Phys. Rev. B* **2006**, *72*, 045411.

(30) Connétable, D.; Rignanese, G. M.; Charlier, J. C.; Blase, X. Room Temperature Peierls Distortion in Small Diameter Nanotubes. *Phys. Rev. Lett.* **2005**, *94*, 015503.

(31) Bohnen, K. P.; Heid, R.; Liu, H. J.; Chan, C. T. Lattice Dynamics and Electron-Phonon Interaction in (3,3) Carbon Nanotubes. *Phys. Rev. Lett.* **2004**, *93*, 245501.